Cancer Letters 455 (2019) 36–47

Contents lists available at ScienceDirect

Cancer Letters

journal homepage: www.elsevier.com/locate/canlet

Original Articles

LYRM2 directly regulates complex I activity to support tumor growth in colorectal cancer by oxidative phosphorylation

Qi Huang[a,b,c,1], Zhigang Chen[a,b,1], Pu Cheng[b,d,1], Zhou Jiang[a,b], Zhen Wang[a,b], Yucheng Huang[e], Chenghui Yang[a,b], Jun Pan[a,b], Fuming Qiu[b,f], Jian Huang[a,b,*]

[a] Department of Surgical Oncology, Second Affiliated Hospital, Zhejiang University School of Medicine, Hangzhou, 310009, China
[b] Key Laboratory of Tumor Microenvironment and Immune Therapy of Zhejiang Province, Hangzhou, 310009, China
[c] Department of Oncology, The Second Affiliated Hospital of Anhui Medical University, Hefei, 230601, China
[d] Department of Gynecology, Second Affiliated Hospital, Zhejiang University School of Medicine, Hangzhou, 310009, China
[e] Department of Chemistry and Biochemistry, University of California, Los Angeles, Los Angeles, CA, 90095, USA
[f] Department of Medical Oncology, Second Affiliated Hospital, Zhejiang University School of Medicine, Hangzhou, 310009, China

ARTICLE INFO

Keywords:
Cancer proliferation
LYRM2
ECT
Complex I
AKT
OXPHOS

ABSTRACT

Oxidative phosphorylation (OXPHOS) in cancer has attracted a considerable attention in the past decades, and accumulated evidence has suggested that it plays an important role in tumor proliferation, metastasis and drug resistance. However, the mechanisms involved in these effects are still ambiguous to date. In this study, we found that LYR motif containing 2 (LYRM2), a novel molecule, is up-regulated in colorectal cancer and promotes tumor growth both *in vivo* and *in vitro*. Furthermore, we discovered that LYRM2 locates in the mitochondria, directly interacts with complex I and increases its activity, thus promoting OXPHOS in colorectal cancer cells. More importantly, we identified a new Akt-S58phos-LYRM2-Complex I axis, which is responsible for the LYRM2-induced tumor growth and the activation of OXPHOS in colorectal cancer. Our finding illustrates the role of LYRM2 in regulating tumor metabolism and provides a new potential target for colorectal cancer treatment.

1. Introduction

Oxidative phosphorylation (OXPHOS) is a metabolic pathway in mitochondria. Cells can use enzymes to oxidize nutrients and generate adenosine triphosphate (ATP) via OXPHOS. A meta-analysis summarized that the average contribution of OXPHOS to ATP production is 83% in cancer cells [1]. It has been reported that cancer cells are relying on OXPHOS to support tumor growth [2,3]. Increasing evidence has demonstrated that OXPHOS inhibitors can effectively target certain cancer subtypes including melanoma, thyroid cancer and endometrial carcinoma [3,4]. OXPHOS can also activate oncogenic pathways like Erk1/2 pathway to promote cancer cell proliferation [5]. Besides, OXPHOS is demonstrated to play a pivotal role in cancer metastasis and drug resistance. Actually, a strong correlation has been revealed between OXPHOS in human invasive breast cancer cells and distant metastases [6]. Colon cancer cells can survive and show resistance to 5-fluorouracil through OXPHOS pathway [2]. Thus, OXPHOS plays an important role in the tumorigenesis and progression of cancer.

Complex I, the first and largest multi-subunit complex in the electron transport chain (ETC), oxidizes nicotinamide adenine dinucleotide (NADH) to create a proton gradient, which drive ATP synthesis [7]. Complex I has been reported to exert a pro-tumorigenic effect on several tumors, including melanoma, breast cancer and osteosarcoma. It can interact with CD147 or STAT3, and activate its activity, therefore promoting the development of cancer [8–10]. Inhibitors of complex I, such as metformin and BAY87-2243, have already been identified as effective anticancer agents [11,12]. On the other hand, mutation of ND1 or ND5, a subunit of complex I, is associated with cancer progression [13–15]. But the role of complex I in colorectal cancer is still undefined.

OXPHOS can be regulated by various genetic alternations, including Rb1 loss [16], Stat3 [17], Chchd2 [18] or Slirp [19] expression, and Akt

Abbreviations: ATP, adenosine triphosphate; ECAR, extracellular acidification rate; ETC, electron transport chain; HE, hematoxylin-eosin; LYRM2, LYR motif containing 2; LYRMs, LYR motif proteins; MS, mass spectrometry; NADH, nicotinamide adenine dinucleotide; OCR, oxygen consumption rates; OXPHOS, oxidative phosphorylation; qRT-PCR, quantitative real-time polymerase chain reaction; TCA, tricarboxylic acid

* Corresponding author. Department of Surgical Oncology, Second Affiliated Hospital, Zhejiang University School of Medicine, Hangzhou, 310009, China.
E-mail address: drhuangjian@zju.edu.cn (J. Huang).

[1] Qi Huang, Zhigang Chen and Pu Cheng contributed equally to this work.

https://doi.org/10.1016/j.canlet.2019.04.021
Received 16 January 2019; Received in revised form 31 March 2019; Accepted 15 April 2019

[20] activation. In our previous study, we have found that a novel molecule LYRM2 is highly expressed in colorectal cancer [21]. LYRM2 is an evolutionarily conserved gene which belongs to LYR (leucine-tyrosine-arginine) motif proteins (LYRMs) family. To date, eleven LYRMs have been found in the human genome and all contain the tripeptide L-Y-R sequence in N-terminal. LYRMs play important roles in regulating mitochondrial metabolism. They can serve as the subunit of mitochondrial complexes like LYRM3 [22] and LYRM6 [23]) or assembly factors including LYRM7 [24], LYRM8 [25], ACN9 [26] and FCM1 [27]. Abnormal expression or mutation of LYRMs implicated in various situations and diseases such as insulin resistance [28], infantile leukoencephalopathy [25], HIV-1 infection-mediated T cell apoptosis [29], breast cancer [30] and esophageal squamous carcinoma [31]. However, the exact function of LYRM2 remains unknown.

In this study, we identified that LYRM2 locates in mitochondria, and increases the activity of mitochondrial complex I and OXPHOS via interacting with complex I in colorectal cancer cells. Moreover, we discovered that an Akt-S58phos-LYRM2-Complex I axis can be responsible for LYRM2-induced proliferation and the activation of OXPHOS.

2. Materials and methods

2.1. Bioinformatic analysis

To identify the LYRM2 expression in human colorectal cancer, data was downloaded from the Oncomine Platform (https://www.oncomine.com) to analyze LYRM2 expression. We also used the online bioinformatics phosphorylation predictor Scansite 4.0 (http://scansite4.mit.edu/4.0/) to predict the phosphorylation sites of LYRM2.

2.2. Mitochondria fractionation

Mitochondria was sub-fractionated by phosphate swelling-shrinking as described before with minor modifications [32,33]. First, the purified mitochondria was suspended in swelling buffer (10 mM KH2PO4, Ph 7.4, adding protease and phosphatase inhibitors) and incubated on ice for 20min with gentle mixing; Second, the prior mitochondria was mixed with equal volume of shrinking buffer (10 mM KH2PO4, pH 7.4, 32% sucrose, 30% glycerol, 10 mM $MgCl_2$, adding protease and phosphatase inhibitors) on ice for another 20min. The last step was centrifugation: the suspension was centrifuged at 10,000 g for 10min, the supernatant contained outer membrane and intermembrane-space fractions (OM&IMS), the pellets contained inner membrane and matrix fractions (IM&MA). We further fractionated OM&IMS by centrifugation at 150,000 g for 1 h at 4 °C. The supernatant and pellets were collected as IMS and OM, respectively. The IMS supernatant was finally concentrated using Microcon 10 K centrifugal filters (Millipore).

2.3. Measurement of oxygen consumption rate (OCR)

The mitochondrial OXPHOS function of cells was measured by a Seahorse XF-96 Extracellular Flux Analyzer (Seahorse Bioscience). Cells were plated on a Seahorse 96-well assay plate at 15,000 cells per well overnight. After calibration of the assay plate using the XF96 software, cells were loaded onto the instrument and subjected to a standard mitochondrial stress test protocol. To test OCR with in intact cells, experiment was performed in medium consist of 10 mM glucose, 1 mM pyruvate and 2 mM glutamine in XF base medium, pH 7.4, at 37 °C. Oligomycin A (an ATP synthase inhibitor; final concentration, 1 μM), carbonylcyanidem-chlorophenylhydrazone (FCCP; a mitochondrial uncoupler; final concentration, 1 μM), antimycin A (complex III inhibitor; final concentration, 0.5 μM) and rotenone (complex I inhibitor; final concentration, 0.5 μM) were added into different ports of the Seahorse cartridge. Total protein of each well was quantified for normalization after the assay. Each experimental group was performed by four or five replicates. O_2 consumption rates (pmol/min/10,000 cells) were measured and calculated as described previously.

2.4. Complex enzyme activity

Complex I enzyme activity assay kit (ab109721, Abcam) was used to measure the mitochondrial OXPHOS complex I enzyme activity. Complex IV and Complex V activity was measured using the assay respectively (ab109911, ab109714, Abcam). The absorbance measurement was conducted on SpectraMax i3 (Molecular Devices).

2.5. Kinase assay in vitro

Akt kinase assays were carried out according to the manufacturer's protocol (Signal Chem). As shown in our experiment, HA-tagged WT or S58A mutant LYRM2 plasmids were transfected in RKO cells. Cells were lysed and incubated with anti-HA-tag antibody, followed by protein G magnetic beads. Next, samples were incubated with 50 ng of active recombinant Akt for 20 min at 30 °C in buffer V containing 5 mM MOPS (pH 7.2, 2.5 mM glycerolphosphate, 5 mM $MgCl_2$, 1 mM EGTA, 0.4 mM EDTA, 0.25 mM DTT, and 200M ATP). The reaction was stopped by adding SDS loading buffer and boiling for 5min. The phosphorylation of substrates was tested by Akt cons antibody (RxxS/T) and HA-tag antibody.

2.6. Mouse xenograft experiments

Four weeks old male nude mice was purchased from the Shanghai Laboratory Animal Center (Chinese Academy of Sciences) and maintained in controlled temperature (23–25 °C) and lighting (8:00 a.m. to 8:00 p.m. light, 8:00 p.m. to 8:00 a.m. dark) at the Laboratory Animal Research Center of Zhejiang Traditional Chinese Medicine University. All experiments were carried out in accordance with the Guide for the Care and Use of Animals for research purposes, and were approved by the Animal Ethics Committee of Zhejiang University.

Mice were randomly divided into 4 groups and injected RKO-L2HA, RKO-CHA, Y-SH1KD and Y-GPH cells (0.2 ml containing 1×10^6 cells) s.c. into the axillary cavity of mice for analyzing their ability to initiate tumor xenografts. The width and length of superficial tumors was measured at the indicated time intervals, and tumor volumes were calculated according to the formula $Vol = 1/2 \times length \times width^2$. After 6 weeks, the mice were anesthetized and placed in a small animal Kodak In-Vivo Imaging System (Kodak, Rochester, NY) for EGFP optical imaging ($\lambda ex = 470$ nm, $\lambda ex = 535$ nm). Molecular Imaging Software VERSION 5.0 (Kodak, Rochester, NY) was used for imaging and data processing to measure the photons per square millimeter (Net P/s/mm, photons/mm^2) of the tumor sites. In addition, the mice xenografts were measured by ultrasonography. Then the xenograft tumors were harvested for further study.

3. Results

3.1. LYRM2 is up-regulated in human colorectal cancer

To analyze the LYRM2 expression pattern in human colorectal cancer tissues, we searched online databases and included three data sets including Kaiser Colon (GSE5206), Skrzypczak Colorectal (GSE20916) and Sabates-Bellver Colon (GSE8671). In these datasets, we found that LYRM2 expression is increased in human colorectal cancer tissues compared to normal tissues (Fig. 1A, B, C). To validate the results in paired fresh colorectal cancer tissues and normal epithelium of patients, we further employed quantitative real-time polymerase chain reaction (qRT-PCR) to measure LYRM2 mRNA expression in 46 paired samples from the Second Affiliated Hospital of Zhejiang University School of Medicine (Supplementary Table 1). Consistent with the online datasets, LYRM2 mRNA expression is significantly higher in tumor samples (Fig. 1D). However, the commercial antibodies

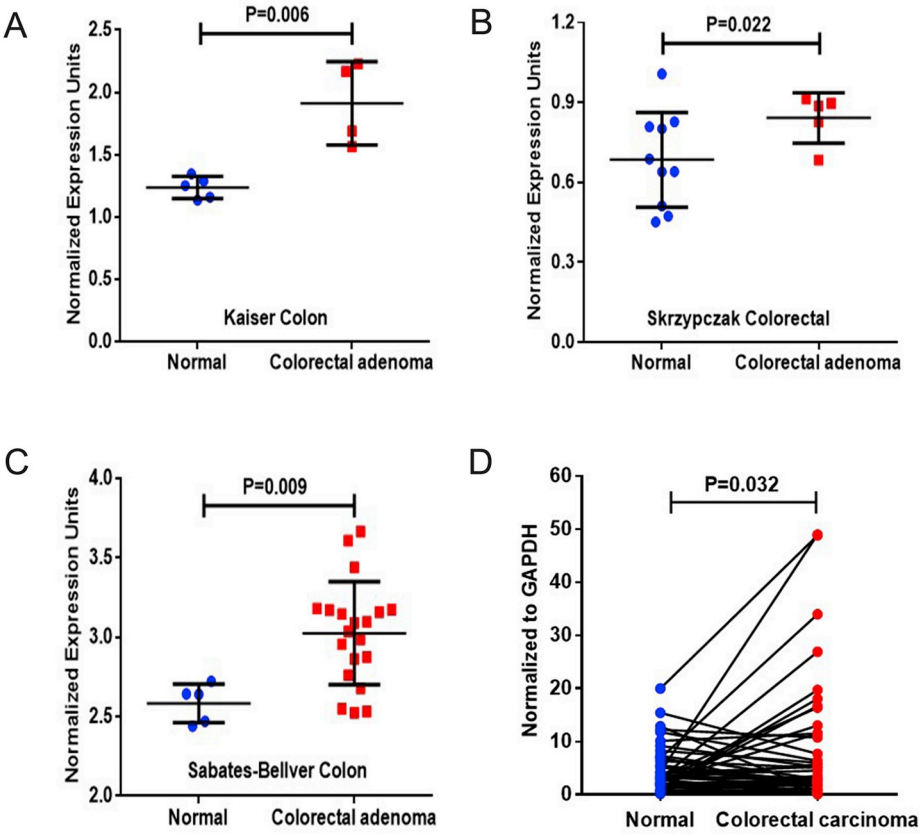

Fig. 1. LYRM2 is up-regulated in human colorectal cancer. **A** Kaiser Colon sets (GSE5206) **B** Skrzypczak Colorectal sets (GSE20916) and **C** Sabates-Bellver Colon sets (GSE8671) were collected to analyze LYRM2 expression pattern in colorectal cancer and normal tissues. **D** QRT-PCR analysis of LYRM2 mRNA expression in 46 paired colorectal cancer and adjacent non-tumor tissue samples (mean ± SEM; n = 46).

against LYRM2 lacked specificity. We did not verify the protein level of LYRM2 in human samples. These results suggested that LYRM2 is up-regulated in colorectal cancer.

3.2. LYRM2 locates in the mitochondrial inner membrane and matrix

Most LYRMs have been reported to locate in mitochondria, such as LYRM3 [34], LYRM4 [35] and LYRM6 [23]. It has been suggested that LYRM2 may also be a mitochondrial protein based on the protein-protein interaction discovered using affinity enrichment mass spectrometry [36]. To identify the location of LYRM2 in tumor cells, we constructed a lentiviral vector of LYRM2 with HA-tag at its C-terminal (L2HA) and used HA antibody to trace LYRM2. In addition, we chose a Mito-Tracker probe to label the mitochondria in cells. As expected, we found that LYRM2 located in the mitochondria of colorectal cancer cells (RKO, SW480) and normal HEK293 cells (Fig. 2A). Moreover, we isolated the mitochondria component from these cells and performed western blotting to further verify the location of LYRM2. HA-tag expression was only detected in the mitochondria component (Fig. 2B and C). These results suggested that, both in cancer cells and normal cells, LYRM2 locates in mitochondria.

To analyze the sub-location of LYRM2 in mitochondria, we divided the mitochondria into three parts: outer membrane, intermembrane-space, and inner membrane plus matrix. As shown in Fig. 2D, we found that LYRM2 located solely in the mitochondrial inner membrane plus matrix part.

3.3. LYRM2 promotes OXPHOS in colorectal cancer cell

Given that LYRM2 locates in mitochondria, we ask whether the aberrant expression of LYRM2 would have an effect on the mitochondrial respiration. Since LYRM2 expression in RKO cells was moderate among colorectal cell lines, it is easier to develop the LYRM2-over-expressed and knock-down stable cell line. Thus, we used RKO for the following functional experiment. As shown in Supplementary Fig. 1A, the LYRM2 mRNA expression in RKO-L2HA cells increased about 20-fold compared to RKO-CHA control cells. The SH1KD functioned effectively and caused nearly 90% reduction of LYRM2 mRNA expression compared to the RKO-GPH control cells. HA-tag antibody was used to detect the exogenous expression of LYRM2 in the following experiments (Supplementary Fig. 1B). As shown in Fig. 3A, the respiratory rate of cells in the 96-well plate increased linearly with the density of cells. It demonstrated that the number of seeded cells was suitable for the respirometry rate assessment. Representative time-dependent changes of the OCR in different groups of cells were shown in Fig. 3B. The over-expression of LYRM2 caused a significant increase of OXPHOS level and altered the cellular responses to the different inhibitors of mitochondrial ETC complexes (including Oligo, an ATP synthase inhibitor; FCCP, a mitochondrial uncoupler; Rotenone, a complex I inhibitor; and Antimycin A, a complex III inhibitor) in colorectal cancer cells. Indexes such as basal respiration, maximal respiration and ATP production in RKO-L2HA cells were significantly higher than those in the control RKO-CHA cells (Fig. 3C). On the other hand, there was a significant decrease in the respiration of RKO-SH1KD cells compared with the control RKO-GPH cells (Fig. 3B and C). Therefore, over-expressed LYRM2 increases the OXPHOS of colorectal cancer cells.

3.4. LYRM2 promotes the growth of colorectal cancer in vitro and in vivo

OXPHOS plays an important role in proliferation of tumor, we asked if LYRM2 promotes the growth of colorectal cancer. To test the effect of LYRM2 on the proliferation of colorectal cancer cells *in vitro*, we employed the cell growth curve and colony formation assay, and tested the expression of proliferation marker Ki67. As shown in Fig. 4A, the growth rate of RKO-L2HA cells significantly increased compared with RKO-CHA cells. From the day 2, the OD values of L2HA cells were significantly higher than those of the RKO-CHA cells ($P \leq 0.001$). In contrast, the OD values of RKO-SH1KD cells were significantly lower

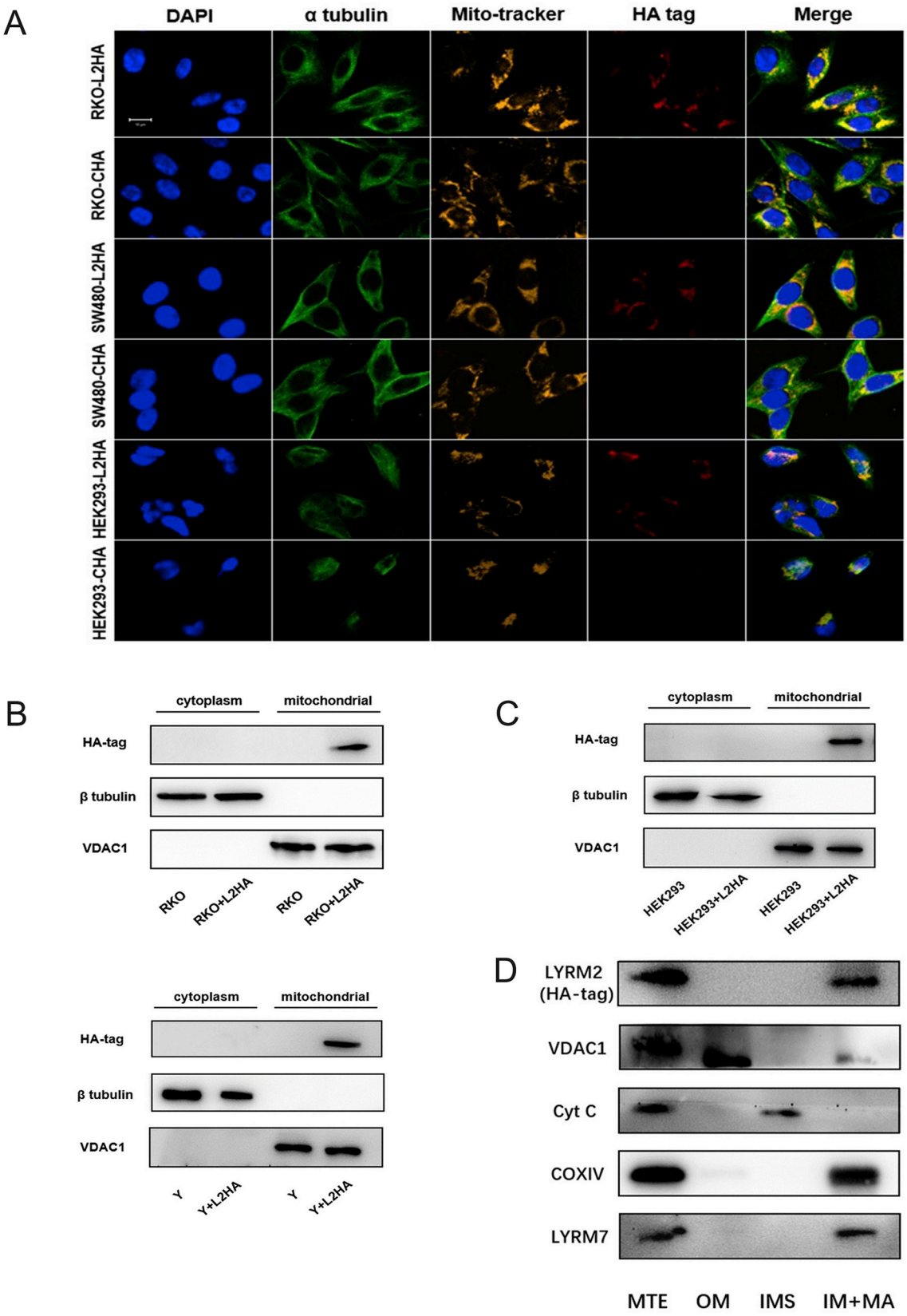

Fig. 2. LYRM2 locates in the mitochondrial inner membrane and matrix. **A** Confocal microscopy of LYRM2 mitochondrial localization. colorectal cancer cells including RKO、SW480 and HEK293 cells transfected with L2HA or control CHA vectors were stained for DNA (DAPI, blue), mito-tracker probe (yellow), α-tubulin (cytoskeleton marker, green) and HA-tag (represent LYRM2, red). Merged images of mitochondrial-localized LYRM2 (the overlap of red with yellow signals) are indicated (Merge). Scale bar, 10 μm. **B** RKO and Y cells transduced with L2HA vectors or wide type cells were fractionated in cytoplasm or mitochondrial extracts and analyzed by western blotting. **C** HEK293 cells transduced with L2HA vectors or wide type cells were fractionated in cytoplasm or mitochondrial extracts and analyzed by western blotting. **D** Mitochondrial extracts (MTE) from RKO cells with stably L2HA expression were further fractionated in outer membrane (OM), intermembrane space (IMS), and inner membrane (IM) + matrix (MA) and analyzed by western blotting. Cyt C: Cytochrome C; VDAC1, Cyt C, COXIV and LYRM7 were identified as the marker of OM, IMS, IM and Matrix separately. (For interpretation of the references to color in this figure legend, the reader is referred to the Web version of this article.)

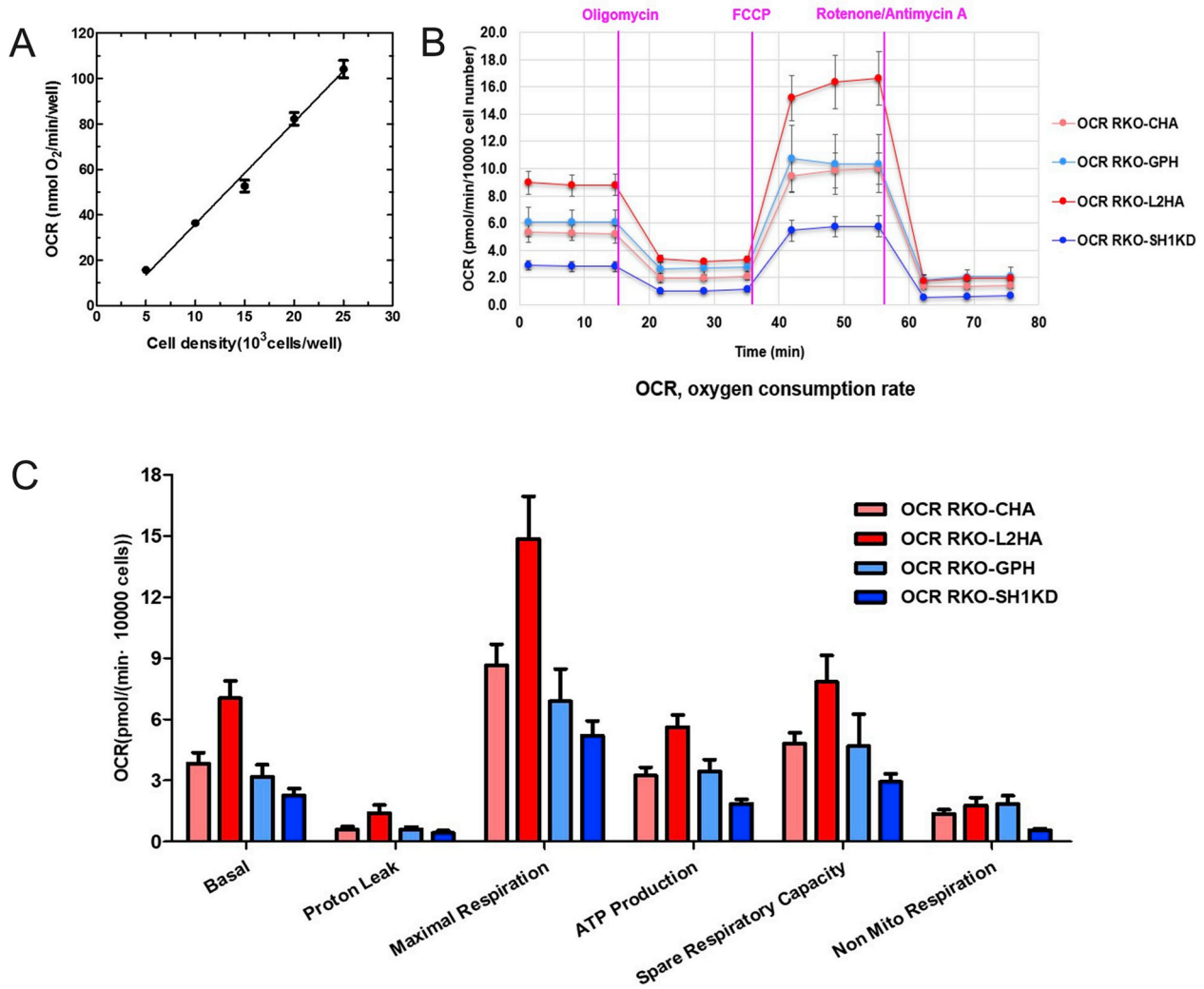

Fig. 3. LYRM2 promotes OXPHOS in colorectal cancer cell. **A** Linear relation between cell density (number of cells plated into well, cells/cm^2) and OCR in corresponding wells(mean ± SEM, n = 3). **B** OCR of RKO cells with L2HA (negative control CHA) or SH1KD (negative control GPH) at baseline and in response to oligomycin, FCCP, and rotenone/antimycin A. Each time-point was shown as an average OCR from at least 6 wells from 3 independent experiments. **C** Quantification of basal respiration, maximal respiration and ATP production from B (mean ± SEM, n = 6).

than the RKO-GPH cells from day 3. In addition, the cells with LYRM2 exogenous overexpression displayed higher expression of Ki67, while the cells with LYRM2 knock-down expressed lower expression of Ki67 than control cells (Fig. 4B). Furthermore, the number of colonies in RKO-L2HA cells increased by 2 folds compared to RKO-CHA cells, and the number of colonies in RKO-SH1KD cells decreased significantly (Fig. 4C). Taken together, LYRY2 promotes the proliferation of colorectal cells *in vitro*.

To analyze the effect of LYRM2 on the proliferation of tumor *in vivo*, we employed a xenograft mice model and used 3 different methods to assess the tumorigenic ability: 1) Since the lentiviral vectors included a GFP tag, we observed the transplanted tumor using GFP fluorescence under an *in vivo* image system. As shown in Fig. 4D, the fluorescence intensity of L2HA xenografts was significantly higher than that in CHA groups, while the fluorescence intensity of SH1KD xenografts was notably lower than it in GPH groups. 2) To assess the volumes of xenografts, we used ultrasonography and found that the tumor volume of L2HA groups was larger than CHA groups, while SH1KD groups developed smaller tumors than GPH groups (Fig. 4E and F). 3) The volume of xenografts was assessed by the widths and lengths of tumors each 5 day until the mice were sacrificed. The data showed that the growth rate of L2HA groups increased significantly while the growth rate of SH1KD groups decreased when compared with their corresponding control groups (Fig. 4G, H, I, J). All the pathological verifications of tumor tissues were conducted using hematoxylin-eosin (HE) staining (Supplementary Fig. 1C). Taken together, LYRM2 promotes the growth of colorectal cancer cells both *in vitro* and *in vivo*.

3.5. LYRM2 interacts complex I to regulate OXPHOS in colorectal cancer

Up-regulation of mitochondrial ETC, or the activation of ETC activity causes the increase of OXPHOS. ETC transfers electrons harvested from the tricarboxylic acid (TCA) cycle on the mitochondrial inner membrane coupled to proton translocation out of the mitochondrial matrix. Three proton-translocating enzymes of the ETC, including complex I, III and IV, generate a proton motive force, which in turn drives ATP synthase (also known as complex V) [37]. We, therefore, checked each mitochondrial ETC protein in RKO-L2HA cells. We isolated complex I-V from cells and detected LYRM2-HA only in the complex I compounds (Fig. 5A). Tandem mass spectrometry (MS) was then conducted to identify the protein components immune-captured by complex I antibodies in RKO-L2HA cells. The assembled subunits of complex I, such as NDUFS1、NDUFS3 and NDUFB9, were detected in these components. In addition, we also found three LYRM2 peptides existed in these components (Fig. 5B, Supplementary Table 2). These two experiments indicated that LYRM2 interacted with complex I in

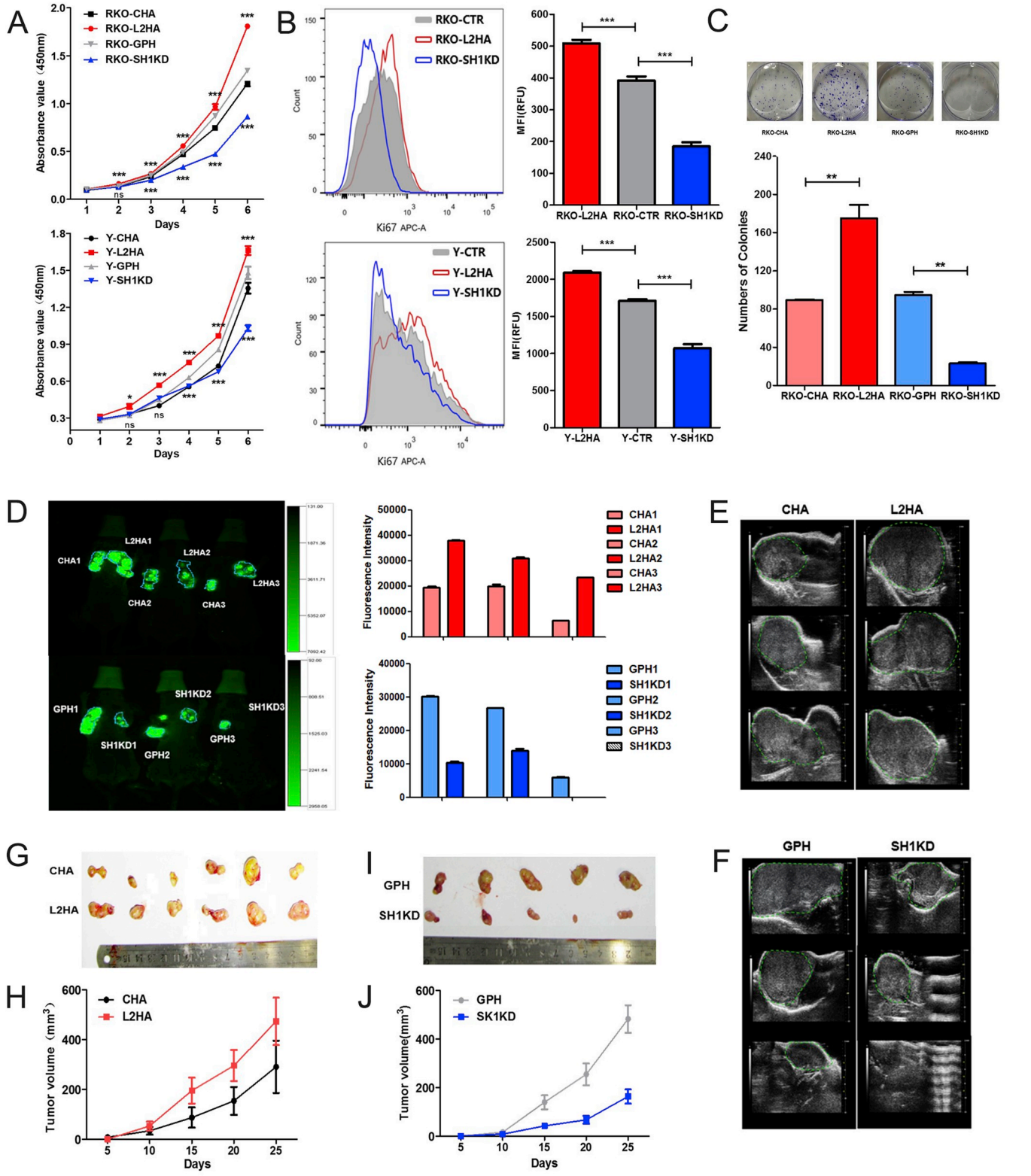

Fig. 4. LYRM2 promotes the growth of colorectal cancer *in vitro* and *in vivo*. **A** RKO (top) and Y (bottom) cells stably transduced with HA-tagged LYRM2 (L2HA) (negative control CHA) or LYRM2-shRNA SH1KD (negative control GPH) were analyzed for cell proliferation by cell counting kit-8 (CCK-8) assay (mean ± SEM; n = 6). **B** Flow cytometry analysis (left) and statistical data (right) of proliferation marker Ki67 level in RKO and Y cells stably transduced with L2HA, SH1KD, and control cells (mean ± SEM; n = 3). MFI: the mean of fluorescence intensity; RFU: relative fluorescence units. **C** RKO cells stably transduced with L2HA, SH1KD, and control cells were analyzed for colony formation after 14 days (top) and the colonies were finally quantified (bottom) (mean ± SEM; n = 3). **D-J** RKO cells transduced with L2HA (control CHA) and Y cells transduced with SH1KD (control GPH) were injected subcutaneously (s.c.) in the axillary cavity of male nude mice (three mice/group; two tumors/mouse). After 6 weeks of tumorigenesis, the GFP fluorescence (D left) in transplanted tumors was observed using an *in vivo* image system and assessed by fluorescence intensity (D right). E、F showed the typical ultrasonic images of xenografts from different groups. G-J showed the representative images of tumors from mice after 6 weeks of tumorigenesis (G、I) and tumor growth (H、J) quantified with a caliper at the indicated time intervals for 5 days (mean ± SEM, n = 3 mice per group). *P < 0.05; **P < 0.01; ***P < 0.001, indicating statistical significance of the observed differences.

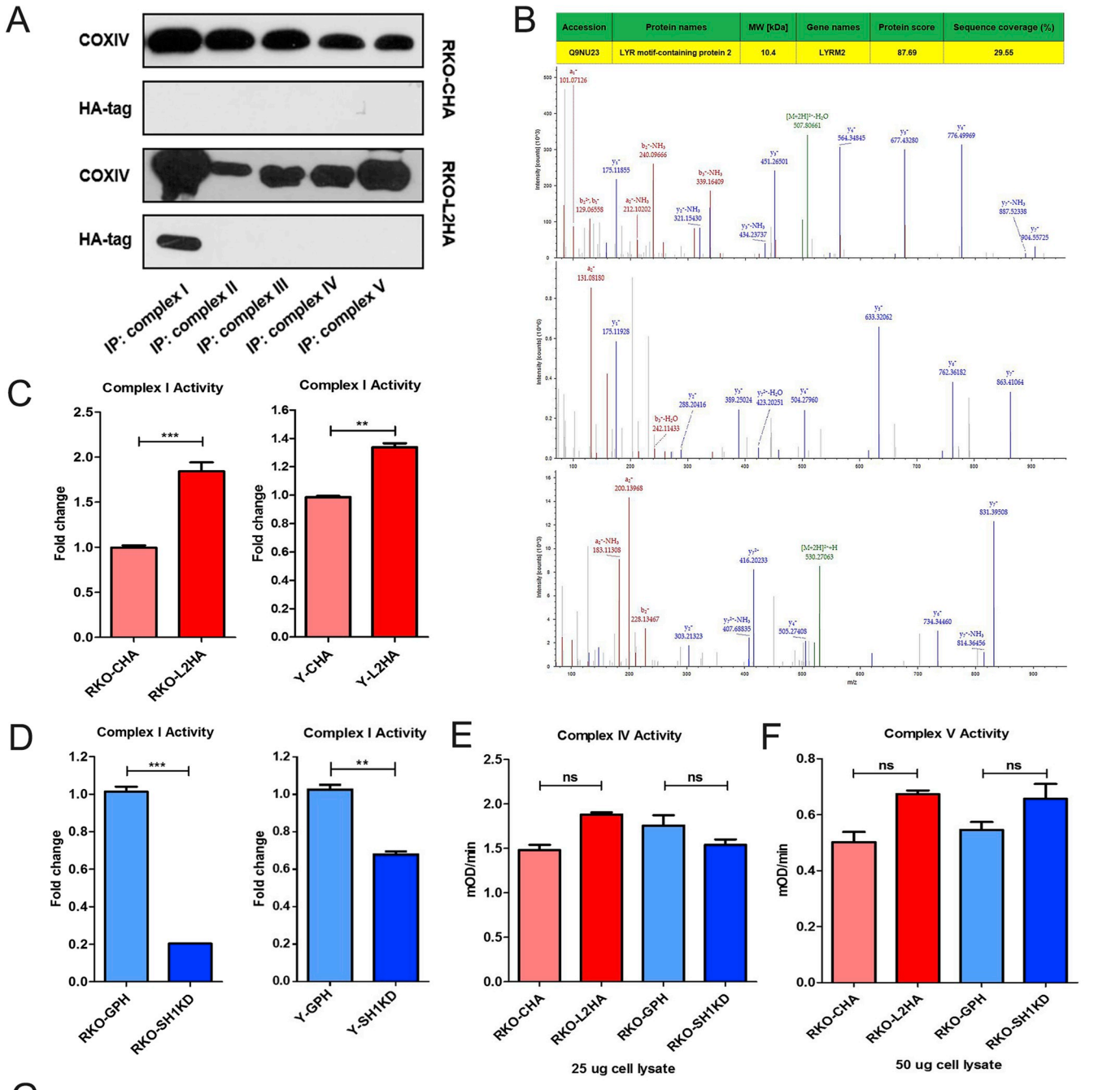

(caption on next page)

Fig. 5. LYRM2 interacts complex I to regulate OXPHOS in colorectal cancer. **A** RKO cells transfected with L2HA or control CHA vector were immunoprecipitated by complex I-V immunocapture antibodies respectively, the immune complexes were analyzed by western blotting. **B** RKO cells transfected with L2HA vector were immunoprecipitated by complex I immunocapture antibody and the immune complexes were analyzed by MS analysis. Three peptides of LYRM2 were found in these immunoprecipitated proteins. **C, D** NADH oxidation by immunocaptured complex I of different cell lysates, expressed as fold-change from control cells (mean ± SEM, n = 3). **E** The activity of complex IV in different cell lysates (25 μg) (mean ± SEM, n = 3). **F** The activity of complex V in different cell lysates (50 μg) (mean ± SEM, n = 3). **G** Cell growth of RKO cells transduced with L2HA or control CHA vectors in the presence of various concentrations of rotenone, a complex I inhibitor. Different concentration of rotenone varying from 12.5 nM to 100 nM suppressed RKO-L2HA cells growth to the same level the RKO-CHA cells reached after rotenone addition (mean ± SEM, n = 6). *P < 0.05; **P < 0.01; ***P < 0.001, indicating statistical significance of the observed differences. ns, not significant.

ETC. Then, we tested whether the expression of LYRM2 had an effect on complex I activity. As shown in Fig. 5C and D, complex I activity increased prominently in the RKO cells with the overexpression of LYRM2 but decreased significantly in the SH1KD cells. Furthermore, we assessed the activity of complex IV and complex V in this respiratory chain, but no significant changes were discovered (Fig. 5E and F). These results suggested that LYRM2 served as an important complex I chaperone, which regulated complex I activity. To test the role of complex I in LYRM2 induced proliferation in colorectal cancer cells, we used rotenone [38], a complex I inhibitor, to block complex I activity in RKO-L2HA and control RKO-CHA cells. The result showed that the growth advantage of RKO-L2HA cells was attenuated after rotenone treatment (Fig. 5G). We concluded that LYRM2 interacts with complex I in mitochondria and promotes its activity, which leads to the high proliferation of colorectal cancer cells.

3.6. LYRM2-complex I interaction is mediated by Akt induced phosphorylation of LYRM2

We further tried to discover the upstream mechanism by which LYRM2 promotes OXPHOS in colorectal cancer cell. The Scansite 4.0 (http://scansite4.mit.edu/4.0/) was utilized to analyze the potential targets and domains of kinases. Nine sites in total were identified during the matching with high thresholds (Fig. 6A). We screened these potential sites with different phosphorylation kinases and found that the LYRM2 sequence surrounding serine at site 58 (S58) matched the Akt consensus phosphorylation site, RxxS/T. To verify this site, we performed the kinase assay and the result showed that active Akt1 or Akt2 phosphorylated LYRM2 (Fig. 6B).

To test the role of Akt signaling pathway in LYRM2 phosphorylation, we constructed a phosphorylation-defective mutant vector (L2HA-S58A:Ser58→Ala). We found that the phosphorylation event occurred only in wild-type L2HA cells but not in the L2HA-S58A phosphorylation-defective mutant cells (Fig. 6B). In addition, we constructed a spontaneous phosphorylation mutant plasmid (L2HA-S58D: Ser58→Asp), which keeps LYRM2 in a spontaneous phosphorylation state. The interaction of LYRM2 and complex I was then checked in the colorectal cancer cells transfected with different mutants and wild-type L2HA. NDUFS1, a complex I subunit, was chosen as a reference of complex I which was maintained constant in wild-type L2HA and L2HA mutants (Fig. 6C). As shown in Fig. 6D, the quantity of LYRM2 combined with complex I reduced significantly in S58A mutant cells. No change was found in S58D mutant cells. The saturation of LYRM2 phosphorylation at S58 might explain the similar phenotype of wild-type and S58D L2HA. Meanwhile, the activity of complex I in S58A mutant cells was similar to that in the control CHA cells (Fig. 6E). These evidences suggested that S58 phosphorylation on LYRM2 involved in the interaction with complex I and the regulation of complex I activity.

Besides, we used a pan-Akt small-molecular inhibitor, MK2206, which fully suppressed the kinase activity of Akt in a concentration dependent manner (Fig. 6F and G). The result showed that the inhibition of Akt was accompanied by the decrease of the combination of LYRM2 with complex I and the activity of complex I in a concentration dependent manner (Fig. 6G and H). Thus, both the mutation of LYRM2 phosphorylation site and the pharmacological Akt inhibitor restrained the interaction between LYRM2 and complex I, and then impaired the complex I activity.

More interestingly, we found that the Akt activity was upregulated markedly in the cells with LYRM2 overexpression, as evidenced by a striking increase in the level of phosphorylated Akt1 and Akt2 while the total Akt protein remained the same (Fig. 6I). Since LYRM2 locates in mitochondria, we supposed that the phosphorylation of LYRM2 by Akt occurs in mitochondria. It has been reported that Akt can be transported into mitochondria in several studies [32,39]. Akt can be recruited to tumor mitochondria during hypoxia and maintained tumor proliferation through phosphorylation [39]. Then, we sub-fractionated mitochondria from RKO-L2HA cells and found that Akt accumulated in mitochondrial outer membrane, inner membrane and matrix, which was consistent with the results of previous studies [32,39]. The phosphorylated Akt was also detected inside mitochondria, and the slender band was only found in inner membrane and matrix part (Fig. 6J). Taken together, these results indicated that both the Akt activation and the downstream LYRM2 phosphorylation events occurred primarily in the inner membrane and matrix part. The interaction of LYRM2 and complex I, which subsequently enhanced complex I activity, is mediated by Akt phosphorylation of LYRM2.

3.7. LYRM2-complex I interaction was verified in human and animal tissues

LYRM2, which could be phosphorylated by activated Akt, was an important regulatory chaperone of complex I. We further validated these *in vitro* data in the tumor tissues from clinical patients and xenograft. We analyzed the relationship between complex I and LYRM2. The LYRM2 mRNA expression was first tested using qRT-PCR, and the rest of the fresh tumors were utilized to analyze the complex I activity. As data shown in Fig. 7B, the complex I activity in colorectal tumor tissues underwent more than two-fold change. Nearly ten-fold change of LYRM2 mRNA expression was found in colorectal tumor tissues compared to normal tissues (Fig. 7A). On the other hand, the complex I activity of the xenograft tumors from *in vivo* assay was analyzed. As shown in the Fig. 7C and D, the complex I activity in the L2HA xenograft was higher than that in CHA control. While, the complex I activity in the SH1KD xenograft was lower than that in GPH control (Fig. 7E and F). Therefore, we proposed an Akt-S58phos-LYRM2-Complex I axis, which regulates the proliferation of colorectal cancer cells through OXPHOS (Fig. 7G).

4. Discussion

In this study, we have shown that LYRM2 locates in mitochondria, interacts with complex I and increases its activity, thus promoting OXPHOS in colorectal cancer cells. More importantly, we confirmed that LYRM2 promotes the phosphorylation of Akt in mitochondria, and the activated Akt, in turn, causes the phosphorylation of LYRM2 at S58 and activates the regulation of the interaction between LYRM2 and complex I. This Akt-S58phos-LYRM2-Complex I axis specifically elucidated the role of LYRM2 in the OXPHOS of colorectal cancer cell. Our above findings have thus filled a major knowledge gap and identified LYRM2 as a novel potential target for blocking OXPHOS in colorectal cancer treatment.

OXPHOS plays an important role in tumor proliferation, metastasis and drug resistance. Previous studies have suggested that tumor cells

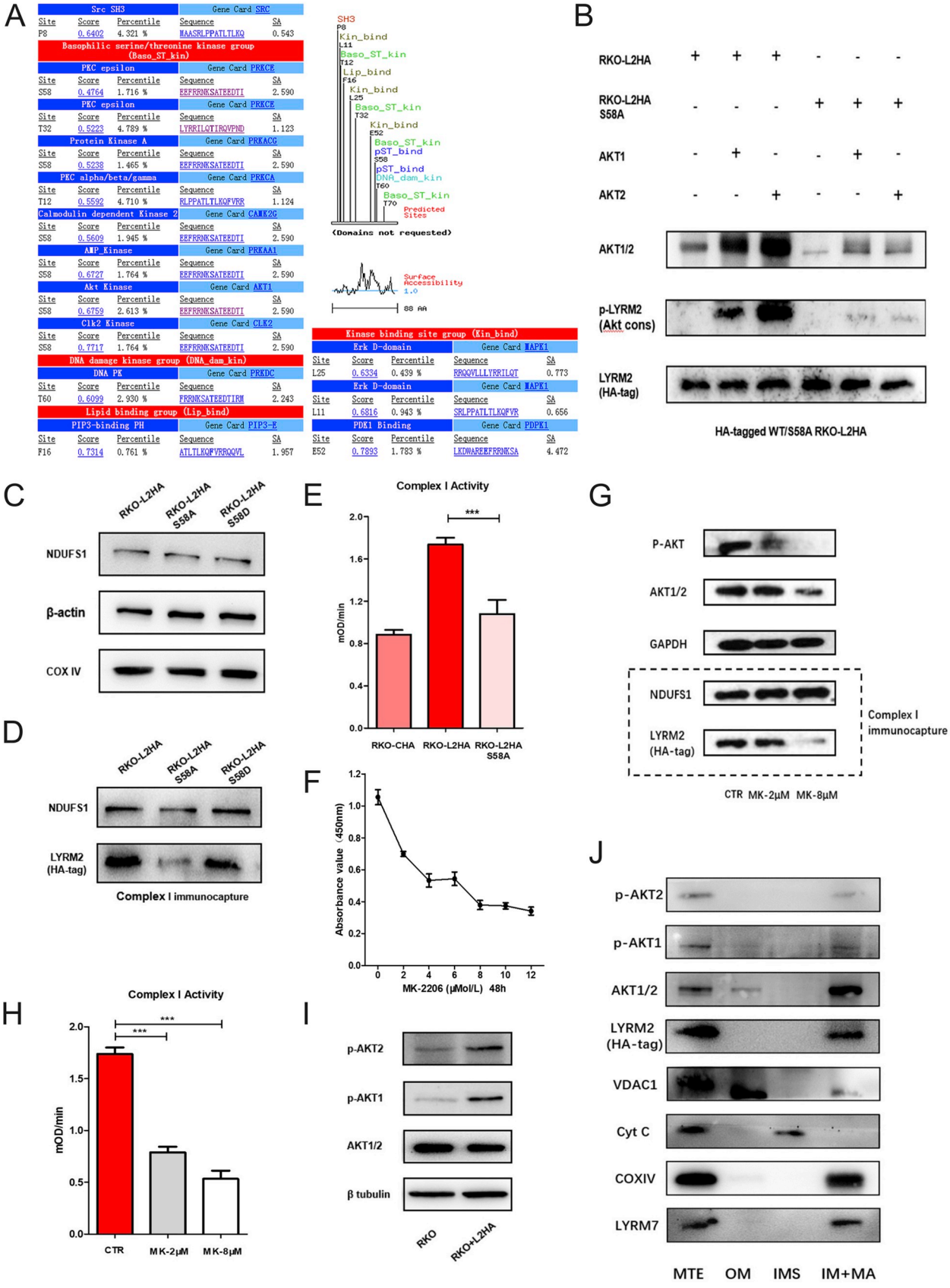

(caption on next page)

Fig. 6. LYRM2-complex I interaction is mediated by Akt induced phosphorylation of LYRM2. **A** Motif scan: predicted sites in peptide map and the surface accessibility using Scansite 3.0 with a high match threshold: residue Ser58 is one of the candidate sites in LYRM2. **B** RKO cells transfected with HA-tagged wide-type LYRM2 or the S58A LYRM2 mutant were immunoprecipitated with HA-tag antibody, and immune complexes were mixed with active Akt1 or Akt2 in a kinase assay followed by western blotting with Akt cons antibody. Akt cons: phospho-Akt substrate (RxxS/T) antibody. **C** NDUFS1 expression in wide type L2HA and L2HA mutants detected by western blotting. **D** RKO cells transfected with HA-tagged wide-type LYRM2 or LYRM2 mutants were immunoprecipitated with complex I immunocaptured antibody, and LYRM2 expression in immune complexes were analyzed by western blotting. **E** Complex I activity was analyzed in RKO cells transfected with wide-type LYRM2 or LYRM2 mutants (mean ± SEM, n = 3). **F** MK2206, a pan-Akt small-molecular inhibitor, was added into L2HA transfected RKO cells to suppress cell proliferation in a concentration dependent manner (mean ± SEM, n = 6). **G** Akt phosphorylation was verified through western blotting after adding different concentration of MK2206 into L2HA transfected RKO cells. Box: Complex I immunocaptured antibody was used to immunoprecipitate proteins in L2HA transfected RKO cells adding different concentration of MK2206, and LYRM2 expression in immune complexes was analyzed by western blotting. **H** Complex I activity was analyzed in L2HA transfected RKO cells adding different concentration of MK2206 (mean ± SEM, n = 3). **I** Akt and phosphorylated Akt expression in RKO wide type and L2HA cells was detected by western blotting. **J** Mitochondrial extracts from RKO cells with stably L2HA expression were further fractionated in OM, IMS, and IM +MA and analyzed by western blotting. p-Akt1, phosphorylated Akt (Ser473); p-Akt2, phosphorylated Akt (Ser474); Cyt C: Cytochrome C; VDAC1, Cyt C, COXIV and LYRM7 were identified as the marker of OM, IMS, IM and MA separately. *P < 0.05; **P < 0.01; ***P < 0.001, indicating statistical significance of the observed differences.

must rely on glycolysis to maintain their proliferation, this phenomenon is named as the famous “Warburg effect” [40]. However, Warburg effect was proposed in the cancer cells with dysfunction of mitochondria [41]. Nowadays, a large number of studies have shown that most tumor cells have normal mitochondrial respiratory capacity [42–44]. Increasing evidence has shown that OXPHOS is up-regulated in many cancers including colorectal cancer, leukemias, lymphomas, pancreatic ductal adenocarcinoma, high OXPHOS subtype melanoma, and endometrial carcinoma [3]. It has been reported that ATP produced by OXPHOS accounts for the majority contribution in certain tumor cells including HeLa, HTB-126, HCC4017, KMS20 and MCF-7 cells [45–48]. In this study, we have also tested the OXPHOS and glycolysis in colorectal cancer cell RKO. The results showed that OXPHOS contributes about 80% ATP in RKO cells, while glycolysis only generates about 20% ATP (Supplementary Fig. 2). Upregulation of OXPHOS can induce the resistance of chemotherapy and promote tumor survival in colorectal tumors via a SIRT1/PGC1α-dependent pathway [49]. Another study had suggested that colon cancer stem cells utilize OXPHOS to produce ATP and maintain their survival by FOXM1/PRDX3 mitochondrial pathway [50]. Hence, inhibition of OXPHOS in tumor cells is a promising approach for cancer treatment [4,51,52]. Researchers had recently reported that IACS-010759, a clinical-grade small-molecule inhibitor of complex I, robustly inhibited tumor growth in models of brain cancer and acute myeloid leukemia [53].

LYRM2 promotes the OXPHOS of colorectal cancer cells. LYRM2 is an evolutionarily conserved gene which belongs to LYRMs family. We found that LYRM2 mRNA is highly expressed in human colorectal cancer for the first time. Because the commercial LYRM2 antibodies were unstable, we can not test the protein level of LYRM2 in human samples. In the following study, we observed that LYRM2 mainly locates in the mitochondrial inner membrane and matrix of cancer cells and HEK293 cells by three different experiments. First, we used HA-tag antibody to detect the exogenous expression of LYRM2 and a Mito-Tracker probe to trace the mitochondria. We found that LYRM2 locates in the mitochondria of colorectal cancer cells and HEK293 cells. Second, we isolated the mitochondria component from these cells and verify LYRM2 locates in the mitochondria component. Third, we divided the mitochondria into three parts: outer membrane, intermembrane-space, and inner membrane plus matrix and tested the location of LYRM2. The results indicated that LYRM2 localized in mitochondrial inner membrane and matrix. These results offered us a hint that LYRM2 may take part in OXPHOS in mitochondria. Next, we use the seahorse respirometry to measure the respiratory rates of cells with different expression of LYRM2. The overexpression of LYRM2 caused an evident increase of OXPHOS. On the other hand, there was a significant decrease in the respiration of RKO-SH1KD cells compared with the control cells. However, the mechanisms that LYRM2 promotes the OXPHOS in colorectal cancer remain unknown.

LYRM2 promotes the OXPHOS by interacting with complex I to regulate complex I activity. The OXPHOS metabolic pathway generates ATP by transporting of electrons to a series of mitochondrial transmembrane complexes. In the mitochondria, three electron-translocating enzymes of the ETC, including complex I, III and IV, generate a proton motive force, which in turn drives ATP synthase through complex V. The electron transferred through complex I was collected from NADH. Complex II can also participate in the electron transporting, but its electron source was FADH2. Thus, we focus on the main ETC: complex I, III, IV and V. We isolated complex I-V from cells and detected LYRM2 interacts the complex I compounds. MS was also used to verify this phenomenon. These two experiments indicated that LYRM2 interacted with complex I in ETC. Since there are over 46 subunits in complex I, we did not identify the definite subunit which is connected with LYRM2 in this study. Complex I is the first and the most elaborate enzyme in the mitochondrial respiratory chain. It has been reported that complex I is hyperactive in human breast cancer cells [54]. We asked whether LYRM2 had an effect on complex I activity. Then we tested the complex I acivity in colorectal cancer cell, xenograft tumor and patients’ fresh tissues. The results showed that complex I activity increased prominently in the samples with overexpressed LYRM2. We also used rotenone, a complex I inhibitor, to block complex I activity in RKO-L2HA, and found that the growth advantage of RKO-L2HA cells was attenuated.

To discover the upstream mechanism by which LYRM2 is regulated in colorectal cancer cells, we used the online database (http://scansite4.mit.edu/4.0/) to analyze the potential domains of kinases. The results showed that the LYRM2 sequence surrounding serine at site 58 (S58) matched the Akt consensus phosphorylation site, RxxS/T. It has been reported that activation of Akt can promote mitochondrial respiration and cellular ATP production [55]. Thus, we tested whether Akt caused the phosphorylation of LYRM2 at S58. We found that Akt can precisely phosphorylate LYRM2 on S58, and phosphorylated LYRM2 then promoted the interaction of LYRM2 and complex I. These data suggested that an auto-regulatory loop may form between Akt and LYRM2, but we only observe an apparent association of imaging signals. We can't unequivocally prove causal and mechanistic interactions. Deeper studies are warranted to rigorously investigate the causal interactions in this auto-regulatory loop. In addition, we found that Akt located in mitochondrial outer membrane, endometrium and matrix. It has been reported that Akt can be detected in mitochondria [39,56,57], but the mechanism by which Akt transfer to mitochondria from cytoplasm is still unknown.

Conflicts and interest

We have no conflicts of interest to declare.

Acknowledgements

J.H. is supported by the National Natural Science Foundation of China (NO.31471391, 81402440 and 81272672) and Zhejiang

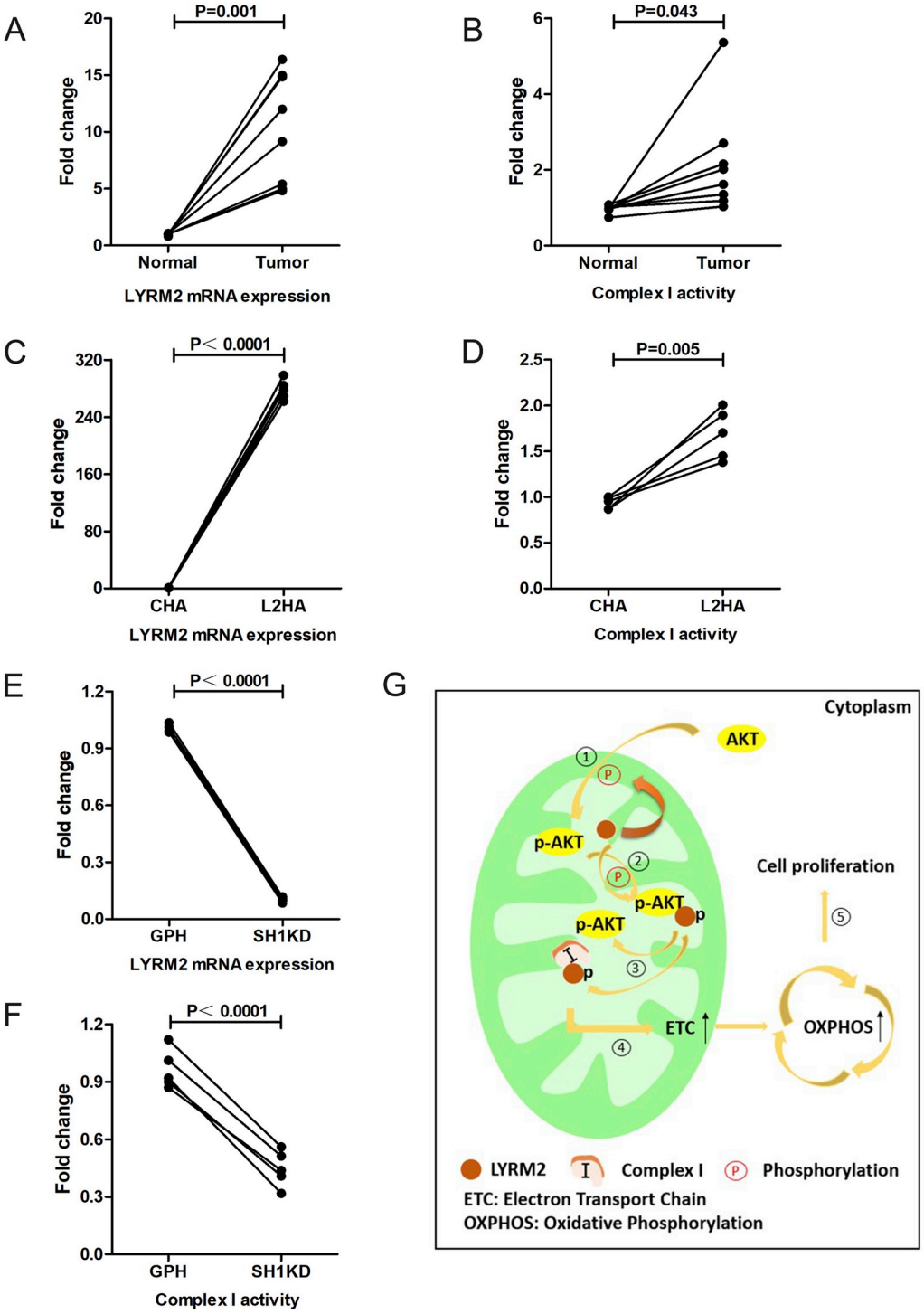

Fig. 7. LYRM2-complex I interaction was verified in human and animal tissues. **A, B** The one-to-one positive correlation of LYRM2 mRNA expression (A) and the complex I activity (B) in individual patient sample. **C-F** The one-to-one positive correlation of LYRM2 mRNA expression (C and E) and the complex I activity (D and F) in xenografted tumor. **G** Schematic model of an Akt-LYRM2-Complex I axis in colorectal cancer cell proliferation.

Provincial Program for the Cultivation of High-Level Innovative Health Talents, Zhejiang provincial key subject of traditional Chinese medicine; Z.C. is supported by National Natural Science Foundation of China (NO.81502564) and Natural Science Foundation of Zhejiang province (NO. LY16H160018, LY18H160001). F.Q. was sponsored by National Natural Science Foundation of China (NO.81472640).

Appendix A. Supplementary data

Supplementary data to this article can be found online at https://doi.org/10.1016/j.canlet.2019.04.021.

References

[1] X.L. Zu, M. Guppy, Cancer metabolism: facts, fantasy, and fiction, Biochem. Biophys. Res. Commun. 313 (2004) 459–465.

[2] C. Denise, P. Paoli, M. Calvani, M.L. Taddei, E. Giannoni, S. Kopetz, et al., 5-fluorouracil resistant colon cancer cells are addicted to OXPHOS to survive and enhance stem-like traits, Oncotarget 6 (2015) 41706–41721.

[3] T.M. Ashton, W.G. McKenna, L.A. Kunz-Schughart, G.S. Higgins, Oxidative phosphorylation as an emerging target in cancer therapy, Clin. Cancer Res. 24 (2018) 2482–2490.

[4] S. Thakur, B. Daley, K. Gaskins, V.V. Vasko, M. Boufraqech, D. Patel, et al., Metformin targets Mitochondrial Glycerophosphate Dehydrogenase (mGPDH) to control Rate of Oxidative Phosphorylation and growth of thyroid cancer in vitro and in vivo, Clin. Cancer Res. 24 (2018) 4030–4043.

[5] C. Zhou, H. Sun, C. Zheng, J. Gao, Q. Fu, N. Hu, et al., Oncogenic HSP60 regulates mitochondrial oxidative phosphorylation to support Erk1/2 activation during pancreatic cancer cell growth, Cell Death Dis. 9 (2018) 161.

[6] V.S. LeBleu, J.T. O'Connell, K.N. Gonzalez Herrera, H. Wikman, K. Pantel, M.C. Haigis, et al., PGC-1alpha mediates mitochondrial biogenesis and oxidative phosphorylation in cancer cells to promote metastasis, Nat. Cell Biol. 16 (2014) 992–1003 1001-1015.

[7] V. Zickermann, S. Kerscher, K. Zwicker, M.A. Tocilescu, M. Radermacher, U. Brandt, Architecture of complex I and its implications for electron transfer and proton pumping, Biochim. Biophys. Acta 1787 (2009) 574–583.

[8] Z. Luo, W. Zeng, W. Tang, T. Long, J. Zhang, X. Xie, et al., CD147 interacts with NDUFS6 in regulating mitochondrial complex I activity and the mitochondrial apoptotic pathway in human malignant melanoma cells, Curr. Mol. Med. 14 (2014) 1252–1264.

[9] K. Szczepanek, Q. Chen, M. Derecka, F.N. Salloum, Q. Zhang, M. Szelag, et al., Mitochondrial-targeted Signal transducer and activator of transcription 3 (STAT3) protects against ischemia-induced changes in the electron transport chain and the generation of reactive oxygen species, J. Biol. Chem. 286 (2011) 29610–29620.

[10] Q. Zhang, V. Raje, V.A. Yakovlev, A. Yacoub, K. Szczepanek, J. Meier, et al., Mitochondrial localized Stat3 promotes breast cancer growth via phosphorylation of serine 727, J. Biol. Chem. 288 (2013) 31280–31288.

[11] W.W. Wheaton, S.E. Weinberg, R.B. Hamanaka, S. Soberanes, L.B. Sullivan, E. Anso, et al., Metformin inhibits mitochondrial complex I of cancer cells to reduce tumorigenesis, eLife 3 (2014) e02242.

[12] L. Schockel, A. Glasauer, F. Basit, K. Bitschar, H. Truong, G. Erdmann, et al., Targeting mitochondrial complex I using BAY 87-2243 reduces melanoma tumor growth, Cancer Metabol. 3 (2015) 11.

[13] H. Kim, T. Komiyama, C. Inomoto, H. Kamiguchi, H. Kajiwara, H. Kobayashi, et al., Mutations in the mitochondrial ND1 gene are associated with postoperative prognosis of localized renal cell carcinoma, Int. J. Mol. Sci. 17 (2016).

[14] M. Akouchekian, M. Houshmand, M.H. Akbari, B. Kamalidehghan, M. Dehghan, Analysis of mitochondrial ND1 gene in human colorectal cancer, J. Res. Med. Sci.: Off. J. Isfahan Univ. Med. Sci. 16 (2011) 50–55.

[15] E.M. Kim, J.K. Park, S.G. Hwang, W.J. Kim, Z.G. Liu, S.W. Kang, et al., Nuclear and cytoplasmic p53 suppress cell invasion by inhibiting respiratory complex-I activity via Bcl-2 family proteins, Oncotarget 5 (2014) 8452–8465.

[16] E. Zacksenhaus, M. Shrestha, J.C. Liu, I. Vorobieva, P.E.D. Chung, Y. Ju, et al., Mitochondrial OXPHOS induced by RB1 deficiency in breast cancer: implications for anabolic metabolism, stemness, and metastasis, Trends Canc. 3 (2017) 768–779.

[17] J. Wegrzyn, R. Potla, Y.J. Chwae, N.B. Sepuri, Q. Zhang, T. Koeck, et al., Function of mitochondrial Stat3 in cellular respiration, Science 323 (2009) 793–797.

[18] Y. Wei, R.N. Vellanki, E. Coyaud, V. Ignatchenko, L. Li, J.R. Krieger, et al., CHCHD2 is coamplified with EGFR in NSCLC and regulates mitochondrial function and cell migration, Mol. Canc. Res.: MCR 13 (2015) 1119–1129.

[19] J.M. Baughman, R. Nilsson, V.M. Gohil, D.H. Arlow, Z. Gauhar, V.K. Mootha, A computational screen for regulators of oxidative phosphorylation implicates SLIRP in mitochondrial RNA homeostasis, PLoS Genet. 5 (2009) e1000590.

[20] Z.P. Shaik, E.K. Fifer, G. Nowak, Akt activation improves oxidative phosphorylation in renal proximal tubular cells following nephrotoxicant injury, American journal of physiology, Ren. Physiol. 294 (2008) F423–F432.

[21] Y.K. Wang, Y.L. Zhu, F.M. Qiu, T. Zhang, Z.G. Chen, S. Zheng, et al., Activation of Akt and MAPK pathways enhances the tumorigenicity of CD133+ primary colon cancer cells, Carcinogenesis 31 (2010) 1376–1380.

[22] T.B. Haack, F. Madignier, M. Herzer, E. Lamantea, K. Danhauser, F. Invernizzi, et al., Mutation screening of 75 candidate genes in 152 complex I deficiency cases identifies pathogenic variants in 16 genes including NDUFB9, J. Med. Genet. 49 (2012) 83–89.

[23] H. Angerer, M. Radermacher, M. Mankowska, M. Steger, K. Zwicker, H. Heide, et al., The LYR protein subunit NB4M/NDUFA6 of mitochondrial complex I anchors an acyl carrier protein and is essential for catalytic activity, Proc. Natl. Acad. Sci. U. S. A. 111 (2014) 5207–5212.

[24] F. Invernizzi, M. Tigano, C. Dallabona, C. Donnini, I. Ferrero, M. Cremonte, et al., A homozygous mutation in LYRM7/MZM1L associated with early onset encephalopathy, lactic acidosis, and severe reduction of mitochondrial complex III activity, Hum. Mutat. 34 (2013) 1619–1622.

[25] D. Ghezzi, P. Goffrini, G. Uziel, R. Horvath, T. Klopstock, H. Lochmuller, et al., SDHAF1, encoding a LYR complex-II specific assembly factor, is mutated in SDH-defective infantile leukoencephalopathy, Nat. Genet. 41 (2009) 654–656.

[26] U. Na, W. Yu, J. Cox, D.K. Bricker, K. Brockmann, J. Rutter, et al., The LYR factors SDHAF1 and SDHAF3 mediate maturation of the iron-sulfur subunit of succinate dehydrogenase, Cell Metabol. 20 (2014) 253–266.

[27] L. Lefebvre-Legendre, J. Vaillier, H. Benabdelhak, J. Velours, P.P. Slonimski, J.P. di Rago, Identification of a nuclear gene (FMC1) required for the assembly/stability of yeast mitochondrial F(1)-ATPase in heat stress conditions, J. Biol. Chem. 276 (2001) 6789–6796.

[28] S. Higashi, K. Katagi, N. Shintani, K. Ikeda, Y. Sugimoto, S. Tsuchiya, et al., p13 overexpression in pancreatic beta-cells ameliorates type 2 diabetes in high-fat-fed mice, Biochem. Biophys. Res. Commun. 461 (2015) 612–617.

[29] J.S. Ladha, M.K. Tripathy, D. Mitra, Mitochondrial complex I activity is impaired during HIV-1-induced T-cell apoptosis, Cell Death Differ. 12 (2005) 1417–1428.

[30] L.D. Li, H.F. Sun, X.X. Liu, S.P. Gao, H.L. Jiang, X. Hu, et al., Down-regulation of NDUFB9 promotes breast cancer cell proliferation, metastasis by mediating mitochondrial metabolism, PLoS One 10 (2015) e0144441.

[31] Y. Uchikado, H. Inoue, N. Haraguchi, K. Mimori, S. Natsugoe, H. Okumura, et al., Gene expression profiling of lymph node metastasis by oligomicroarray analysis using laser microdissection in esophageal squamous cell carcinoma, Int. J. Oncol. 29 (2006) 1337–1347.

[32] G.N. Bijur, R.S. Jope, Rapid accumulation of Akt in mitochondria following phosphatidylinositol 3-kinase activation, J. Neurochem. 87 (2003) 1427–1435.

[33] B.H. Kang, J. Plescia, T. Dohi, J. Rosa, S.J. Doxsey, D.C. Altieri, Regulation of tumor cell mitochondrial homeostasis by an organelle-specific Hsp90 chaperone network, Cell 131 (2007) 257–270.

[34] C. Hunte, V. Zickermann, U. Brandt, Functional modules and structural basis of conformational coupling in mitochondrial complex I, Science 329 (2010) 448–451.

[35] Y. Shi, M.C. Ghosh, W.H. Tong, T.A. Rouault, Human ISD11 is essential for both iron-sulfur cluster assembly and maintenance of normal cellular iron homeostasis, Hum. Mol. Genet. 18 (2009) 3014–3025.

[36] B.J. Floyd, E.M. Wilkerson, M.T. Veling, C.E. Minogue, C. Xia, E.T. Beebe, et al., Mitochondrial protein interaction mapping identifies regulators of respiratory chain function, Mol. Cell 63 (2016) 621–632.

[37] G. Lenaz, M.L. Genova, Structure and organization of mitochondrial respiratory complexes: a new understanding of an old subject, Antioxidants Redox Signal. 12 (2010) 961–1008.

[38] Q. Xu, E. Biener-Ramanujan, W. Yang, V.K. Ramanujan, Targeting metabolic plasticity in breast cancer cells via mitochondrial complex I modulation, Breast Canc. Res. Treat. 150 (2015) 43–56.

[39] Y.C. Chae, V. Vaira, M.C. Caino, H.Y. Tang, J.H. Seo, A.V. Kossenkov, et al., Mitochondrial Akt regulation of hypoxic tumor reprogramming, Cancer Cell 30 (2016) 257–272.

[40] O. Warburg, On the origin of cancer cells, Science 123 (1956) 309–314.

[41] O. Warburg, F. Wind, E. Negelein, The metabolism of tumors in the body, J. Gen. Physiol. 8 (1927) 519–530.

[42] G. Gentric, V. Mieulet, F. Mechta-Grigoriou, Heterogeneity in cancer metabolism: new concepts in an old field, Antioxidants Redox Signal. 26 (2017) 462–485.

[43] I.A. Barbosa, N.G. Machado, A.J. Skildum, P.M. Scott, P.J. Oliveira, Mitochondrial remodeling in cancer metabolism and survival: potential for new therapies, Biochim. Biophys. Acta 1826 (2012) 238–254.

[44] C. Frezza, E. Gottlieb, Mitochondria in cancer: not just innocent bystanders, Semin. Canc. Biol. 19 (2009) 4–11.

[45] C. Jose, N. Bellance, R. Rossignol, Choosing between glycolysis and oxidative phosphorylation: a tumor's dilemma? Biochim. Biophys. Acta 1807 (2011) 552–561.

[46] R. Moreno-Sanchez, A. Marin-Hernandez, E. Saavedra, J.P. Pardo, S.J. Ralph, S. Rodriguez-Enriquez, Who controls the ATP supply in cancer cells? Biochemistry lessons to understand cancer energy metabolism, Int. J. Biochem. Cell Biol. 50 (2014) 10–23.

[47] M. Guppy, P. Leedman, X. Zu, V. Russell, Contribution by different fuels and metabolic pathways to the total ATP turnover of proliferating MCF-7 breast cancer cells, Biochem. J. 364 (2002) 309–315.

[48] L. Yu, M. Lu, D. Jia, J. Ma, E. Ben-Jacob, H. Levine, et al., Modeling the genetic regulation of cancer metabolism: interplay between glycolysis and oxidative phosphorylation, Cancer Res. 77 (2017) 1564–1574.

[49] T.T. Vellinga, T. Borovski, V.C. de Boer, S. Fatrai, S. van Schelven, K. Trumpi, et al., SIRT1/PGC1alpha-Dependent increase in oxidative phosphorylation supports chemotherapy resistance of colon cancer, Clin. Cancer Res.: Off. J. Amer. Assoc. Canc. Res. 21 (2015) 2870–2879.

[50] I.S. Song, Y.J. Jeong, J. Han, Mitochondrial metabolism in cancer stem cells: a therapeutic target for colon cancer, BMB Rep. 48 (2015) 539–540.

[51] N. Yadav, S. Kumar, T. Marlowe, A.K. Chaudhary, R. Kumar, J. Wang, et al., Oxidative phosphorylation-dependent regulation of cancer cell apoptosis in response to anticancer agents, Cell Death Dis. 6 (2015) e1969.

[52] J. Park, J.K. Shim, J.H. Kang, J. Choi, J.H. Chang, S.Y. Kim, et al., Regulation of Bioenergetics through Dual Inhibition of Aldehyde Dehydrogenase and Mitochondrial Complex I Suppresses Glioblastoma Tumorspheres, Neuro-oncology, 2017.

[53] J.R. Molina, Y. Sun, M. Protopopova, S. Gera, M. Bandi, C. Bristow, et al., An inhibitor of oxidative phosphorylation exploits cancer vulnerability, Nat. Med. 24 (2018) 1036–1046.

[54] D. Whitaker-Menezes, U.E. Martinez-Outschoorn, N. Flomenberg, R.C. Birbe, A.K. Witkiewicz, A. Howell, et al., Hyperactivation of oxidative mitochondrial metabolism in epithelial cancer cells in situ: visualizing the therapeutic effects of metformin in tumor tissue, Cell Cycle 10 (2011) 4047–4064.

[55] R.B. Robey, N. Hay, Is Akt the "Warburg kinase"?-Akt-energy metabolism interactions and oncogenesis, Semin. Canc. Biol. 19 (2009) 25–31.

[56] B. Park, Y.T. Je, K.H. Chun, Akt is translocated to the mitochondria during etoposide-induced apoptosis of HeLa cells, Mol. Med. Rep. 12 (2015) 7577–7581.

[57] X.R. Wang, R. Ding, T.Q. Tao, H.M. Mao, M. Liu, Y.S. Xie, et al., Myofibrillogenesis regulator 1 rescues renal ischemia/reperfusion injury by recruitment of PI3K-dependent P-AKT to mitochondria, Shock 46 (2016) 531–540.